

Continuous Knowledge-Preserving Decomposition for Few-Shot Continual Learning

Xiaojie Li^{1,2} Yibo Yang³ Jianlong Wu¹ David A. Clifton⁴
 Yue Yu² Bernard Ghanem³ Min Zhang¹

¹Harbin Institute of Technology, Shenzhen ²Peng Cheng Laboratory

³King Abdullah University of Science and Technology ⁴University of Oxford

xiaojieli0903@gmail.com, yibo.yang93@gmail.com, wujianlong@hit.edu.cn, davidc@robots.ox.ac.uk

yuy@pcl.ac.cn, bernard.ghanem@kaust.edu.sa, zhangmin2021@hit.edu.cn

https://github.com/xiaojieli0903/cpkd_fscil

Abstract

Few-shot class-incremental learning (FSCIL) involves learning new classes from limited data while retaining prior knowledge, and often results in catastrophic forgetting. Existing methods either freeze backbone networks to preserve knowledge, which largely limits adaptability, or rely on additional modules or prompts, introducing extra inference overhead. To this end, we propose Continuous Knowledge-Preserving Decomposition for FSCIL (CKPD-FSCIL), a framework that efficiently decomposes model’s weights into two complementary parts: one that compacts existing knowledge (knowledge-sensitive components) and another carries redundant capacity to accommodate new abilities (redundant-capacity components). The decomposition is guided by a covariance matrix from replay samples such that the decomposed principal components align closely with the classification abilities of these representative samples. During adaptation, we freeze the knowledge-sensitive components and only adapt the redundant-capacity components, fostering plasticity for new abilities while minimizing interference with existing knowledge, without changing model architecture or increasing inference overhead. Additionally, CKPD introduces an adaptive layer selection strategy to identify layers with the most redundant capacity, dynamically allocating adapters across layers. Experiments on multiple benchmarks demonstrate that CKPD-FSCIL outperforms the state-of-the-art methods.

1. Introduction

Few-shot class-incremental learning (FSCIL) [47] addresses the need to incrementally learn new classes from limited data while preserving previously acquired knowledge. The setting is common in real-world applica-

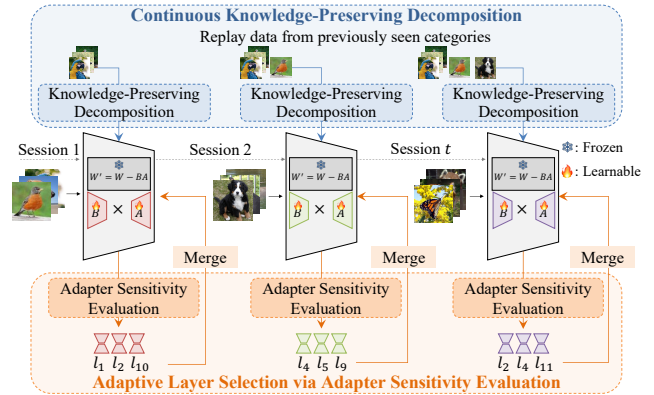


Figure 1. The motivation of CKPD-FSCIL: We utilize replay data from previously seen categories to perform knowledge-preserving decomposition at each session, decomposing network weights into knowledge-sensitive components (frozen during adaptation) and redundant-capacity components (learnable B and A). Adapter sensitivity evaluation is then applied to automatically select layers (l_*). We repeat the steps as session goes on, continuously assimilating new abilities and performing adaptive layer selection.

tions *e.g.*, adaptive recommendation systems and robotics in evolving environments, where models must efficiently adapt to new information without compromising existing knowledge. It combines both demands of few-shot learning [40, 50], which requires learning from limited data, and class-incremental learning [29, 41], which incorporates new classes over time without retraining [49, 65]. This combination presents significant challenges. First, models are susceptible to *catastrophic forgetting*, where knowledge from previous classes is overwritten when learning new classes without access to prior data [13, 33, 61]. Second, the scarcity of data for newly introduced classes increases overfitting risks, hindering generalization [43, 45]. Finally, a delicate balance between maintaining *stability* of

prior knowledge and encouraging *plasticity* to accommodate new information [35] is important but elusive.

Various strategies have been developed to address these challenges. Data replay-based methods [1, 31, 37] store or synthesize data from previous classes to mitigate forgetting. Optimization-based approaches use meta-learning [46], specialized loss functions [22], and geometric constraints [32] to improve learning effectiveness from limited data. Additionally, dynamic adaptation techniques introduce dynamic architectures [57–59], classifiers [47, 53, 63], and parameters [27] to adapt to new classes. Despite these efforts, several limitations remain. The majority of FSCIL methods choose to freeze the backbone network in training because fine-tuning on few-shot data is prone to overfitting and thus exacerbates catastrophic forgetting [18, 27, 47, 60, 70]. However, limited capacity for adaptation will obstruct the acquisition of representative and discriminative features for new tasks. Additionally, some studies introduce task-specific prompts or adapters and only fine-tune them in adaptation [6, 14, 30, 36, 39, 48, 54], yet they introduce additional parameters or inference complexity.

In this paper, we investigate the following question,

Can we decompose the weights of a model into two complementary components such that one compacts the ability of previously acquired knowledge, and the other corresponds to the redundant capacity to spare for new knowledge?

By finding a solution to this question, we can adaptively freeze the component sensitive to existing knowledge while making the redundant component learnable during incremental training. This could fundamentally resolve the dilemma between fully freezing and fine-tuning a backbone network, without changing the model architecture or incurring additional inference overhead. To this end, we propose a **C**ontinuous **K**nowledge-**P**reserving **D**ecomposition (CKPD) framework, which enables us to continuously detach the redundant component from the essential components associated with the already acquired knowledge. The intuition is to perform dimension reduction for the feature space to allocate extra space for new knowledge. Considering that the output feature space of a linear projection in neural networks usually contains larger inter-class variance with smaller intra-class variance [16], the principal components of the covariance matrix projected onto the output space capture the most influential and discriminative elements that contribute to classification [12, 34].

Inspired by this insight, we collect the covariance matrix before a linear layer using the replay strategy that allows storing a few samples of old classes (usually one sample per old class), and perform singular value decomposition (SVD) for the covariance matrix multiplied by the linear projection weight, such that the components with the large singular values most correspond to the classification abili-

ties of these representative samples. Accordingly, the components with small singular values are redundant and we split them away as learnable adapters for new knowledge while freezing the other components to preserve existing knowledge. We multiply the inverse of the covariance matrix to reconstruct the linear projection weight trained on previous classes, so it will not change the weight significantly at the start of each session’s adaptation in continual training. Compared to directly decomposing the weight by SVD into orthogonal components agnostic of any ability of concern, our method concentrates the existing classification abilities associated with the representative samples into the principal components, and thus the remaining components contain more capacity for new knowledge with less interference with the already acquired abilities. Moreover, our method retains inference efficiency by merging the fine-tuned adapters with the frozen components to recover the original model structure, without introducing additional parameters or computation cost at inference.

To capture evolving task characteristics in continual training, we continuously recalculate the covariance matrix based on replay data of previously seen classes to perform our knowledge-preserving decomposition before each session’s adaptation, as shown in the top part of Figure 1. During continuous adaptation, the capacity available for accommodating new knowledge varies across different layers and changes over sessions. Therefore, we further introduce an adaptive strategy for automatic layer selection. Concretely, we perform our knowledge-preserving decomposition for all linear layers and build adapters using the singular vectors with the smallest r singular values. We develop a metric named the Adapter Sensitivity Ratio (ASR), and it is computed as $ASR^l = \frac{\sigma_{-r}^l}{\sigma_{\min}^l}$, where σ_{-r}^l is the r -th last singular value, and σ_{\min}^l refers to the smallest singular value of the l -th layer. The metric evaluates the sensitivity of the detached adapter to existing knowledge. A large ASR indicates that parts of the important components with non-negligible contributions to previously acquired abilities are included into the adapter, while a small value means that the adapter only contains redundant components with similar insignificant contributions and thus less interferes with existing knowledge. We rank ASR^l of all layers and select the top- K layers with the smallest ASR values. By doing so, our method dynamically allocates adapters across layers in each session, as illustrated in the bottom part of Figure 1.

Our contributions can be summarized as follows:

- We propose **CKPD-FSCIL**, a framework that efficiently decompose linear projection weights into complementary components such that the one compacts the ability of previously acquired knowledge and is frozen during training, and the other corresponds to the redundant capacity and is learnable to adapt to new knowledge.

- We develop an adapter sensitivity evaluation strategy for automatic adapter allocation across layers, which further maintains the stability of previously acquired knowledge while ensuring the capacity for learning new tasks.
- Extensive experiments demonstrate that CKPD outperforms state-of-the-art methods on multiple benchmarks. Ablation studies and analyses verify the effectiveness of our methods in fostering adaptability and mitigating catastrophic forgetting.

2. Related Works

2.1. Few-shot Class-Incremental Learning

Few-shot class-incremental learning (FSCIL) [47] combines the goals of few-shot learning [40, 50] and class-incremental learning [29, 41, 49, 65]. It requires training a base model on a comprehensive set of base classes, and incrementally learning new classes from a few examples while retaining prior knowledge, which presents key challenges of catastrophic forgetting [13, 33, 61], data scarcity [43, 45], and stability-plasticity dilemma [35]. Existing approaches tackle these issues through data replay or generation approaches [1, 31, 37], optimization strategies including meta-learning and advanced loss functions [22, 32, 46, 60], and dynamic adaptation methods that adjust model structures or classifiers to accommodate new classes [47, 53, 57–59, 63]. Dynamic weight aims to adapt models based on input characteristics without incrementally increasing overall complexity [27]. However, most methods limit the backbone’s adaptability by freezing it to mitigate catastrophic forgetting, which largely restricts the capacity to accommodate new knowledge [18, 27, 47, 60, 70]. Alternatively, a trainable backbone often leads to overfitting on few-shot samples, worsening catastrophic forgetting [4, 10, 24]. Different from these methods, our method decomposes the linear projection weights in backbone network into complementary parts, one concentrating the existing abilities and the other one providing redundant capacity for learning new knowledge, and thus ensures both stability and plasticity.

2.2. Efficient Adaptation

Parameter-efficient fine-tuning is an effective technique to efficiently adapt a model with only a small number of learnable parameters [9, 56], which is especially instrumental for pre-trained large language models whose full fine-tuning is resource-demanding. Adapter-based [17, 19, 25] and prompt-based methods [21, 26, 28, 55] insert additional modules or learnable prompts and only train them for adaptation. While effective, these approaches generally increase inference costs by adding extra parameters or modifying model architecture. Low-rank adaptation methods, exemplified by LoRA [20], build low-rank matrices as learnable

adapters that can be merged into the pre-trained weights and thus will not cause architectural change or additional inference cost. LoRA has inspired a series of follow-up studies. AdaLoRA [66] adopts adaptive rank in different layers. CorDA [61] proposes a context-oriented decomposition method to initialize the low rank adapters. Compared with CorDA, which adapts a model only once, we deal with evolving task characteristics in continual training, and the capacity available for accommodating new knowledge always varies across different layers and changes over sessions. Therefore, our method differs from CorDA in that we support adaptive layer selection and our adapters can be dynamically allocated in each session.

Efficient adaptation methods are also developed for FSCIL with prompt tuning and adapter mechanisms [6, 14, 30, 36, 39, 48, 48, 54]. PL-FSCIL [48] employs domain and task-specific prompts to adapt a pre-trained vision Transformer (ViT) to new classes incrementally. ASP-FSCIL [30] introduces an attention-aware and self-adaptive prompt framework to retain shared knowledge across tasks. FSPT-FSCIL [39] further refines prompt usage by combining fast-update and slow-update prompts. Additionally, PriViLege [36] and CPE-CLIP [6] utilize pre-trained vision-language Transformers with learnable prompts, while KANet [54] and CA-CLIP [14] employ adapters to integrate new information. However, these methods often introduce additional parameters, increasing inference complexity. As a comparison, our method adopts the low-rank adapter structure and can recover the architecture without incurring extra parameters or inference overhead. Besides, prior methods rely on manual layer selection [30, 39, 54], while our method enables automatic layer selection with adaptive adjustment over sessions.

3. Method

We describe the problem formulation of FSCIL in Sec. 3.1. And then we propose our CKPD-FSCIL, composed of continuous knowledge-preserving decomposition (CKPD) in Sec. 3.2, and adapter sensitivity evaluation for adaptive layer selection in Sec. 3.3. Finally, we specify the implementation details in Sec. 3.4.

3.1. Problem Formulation

FSCIL involves training a model incrementally across multiple sessions, denoted as $\{\mathcal{D}^{(0)}, \mathcal{D}^{(1)}, \dots, \mathcal{D}^{(T)}\}$. In each session t , the model receives a training set $\mathcal{D}^{(t)} = \{(\mathbf{x}_i, y_i)\}_{i=1}^{|\mathcal{D}^{(t)}|}$, where \mathbf{x}_i is an input sample and y_i is its corresponding label. The base session $\mathcal{D}^{(0)}$ provides a comprehensive label set $\mathcal{C}^{(0)}$ with substantial data for each class, serving as the foundation for the model’s initial learning. In subsequent sessions $\mathcal{D}^{(t)}$, $t > 0$, the model is introduced to new classes with only a few labeled images per class,

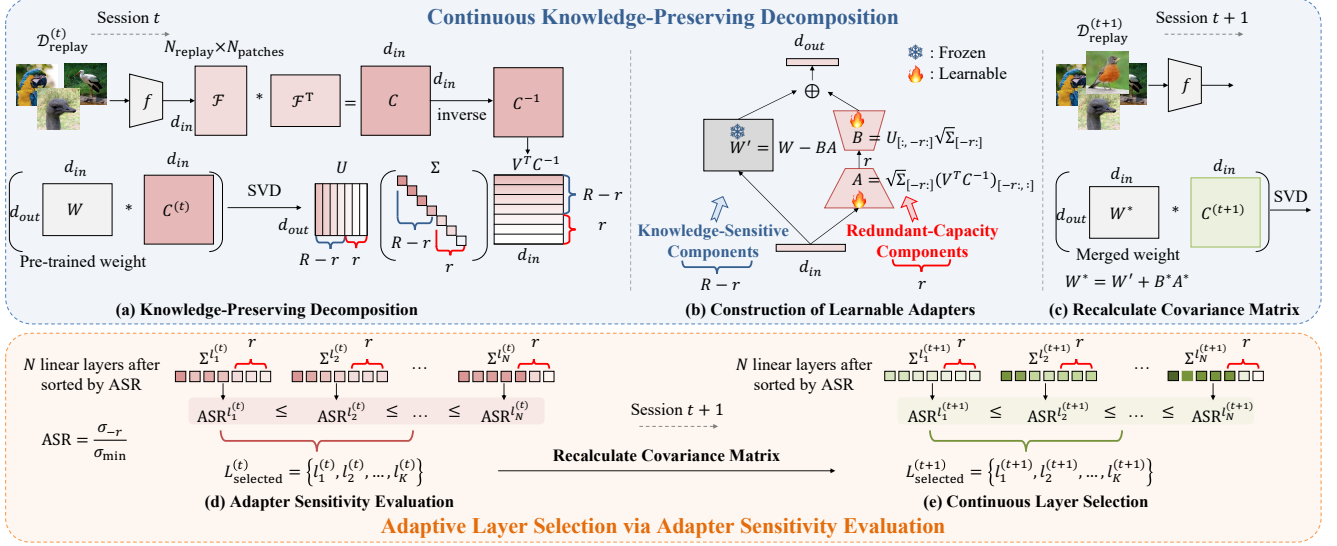


Figure 2. Overview of CKPD-FSCIL. The framework includes: (a) **Knowledge-Preserving Decomposition**, which computes covariance matrices from replay samples to decompose weights into frozen knowledge-sensitive components and learnable redundant-capacity components; (b) **Construction of Learnable Adapters**, where redundant-capacity components are used to form low-rank matrices B and A for new task adaptation, while knowledge-sensitive components are frozen to preserve existing knowledge; (c) **Recalculation of Covariance Matrices**, which updates covariance matrices in each session using the latest replay data; (d) **Adapter Sensitivity Evaluation**, which computes Adapter Sensitivity Ratios (ASR) to identify the K most adaptable layers with the highest redundant capacity and minimal impact on existing knowledge; and (e) **Continuous Layer Selection**, which dynamically recalculates ASR values in each session to update the K most adaptable layers, ensuring efficient adaptation while preserving prior knowledge.

typically following a p -way q -shot setup—meaning p new classes with q samples for each class. Importantly, there is no overlap between the classes of different sessions, *i.e.*, $\mathcal{C}^{(t)} \cap \mathcal{C}^{(t')} = \emptyset$ for all $t' \neq t$. Other than data replay with limited samples, the training data from previous sessions are inaccessible in future sessions. During evaluation in session t , the model is tested on data from all classes encountered, *i.e.*, $\bigcup_{i=0}^t \mathcal{C}^{(i)}$. The goal is to achieve high accuracy across all learned classes, balancing the acquisition of new knowledge with the retention of existing knowledge.

3.2. Continuous Knowledge-Preserving Decomposition

The motivation of CKPD is to decompose linear projection weights into two complementary parts: **knowledge-sensitive components** that compact existing abilities and **redundant-capacity components** that have limited influence on existing abilities and carry redundant capacity to accommodate new knowledge. We achieve this by borrowing ideas from principal component analysis, but decompose covariance matrices projected onto the output feature space of each linear layer, such that the obtained principal components most correspond to the classification abilities of these representative samples. Moreover, we can reconstruct weights by multiplying the inverse of the covariance matrix.

As illustrated in Fig. 2 (a), at the start of each incremen-

tal session $t > 0$, we collect a small subset of replay data, $\mathcal{D}_{\text{replay}}^{(t)} = \{(x_i, y_i) \mid y_i \in \bigcup_{i=0}^{t-1} \mathcal{C}^{(i)}\}$, containing **only one sample** for each old class. These replay samples are passed through the model’s backbone network f to compute activations and calculate covariance matrices $C^{(t)}$ before each linear layer (we omit layer index for simplicity) as follows,

$$C^{(t)} = \frac{1}{N_{\text{replay}}} \mathcal{F}^{(t)} \mathcal{F}^{(t)\top} \in \mathbb{R}^{d_{\text{in}} \times d_{\text{in}}}. \quad (1)$$

where $\mathcal{F}^{(t)} \in \mathbb{R}^{d_{\text{in}} \times N_{\text{replay}} N_{\text{patch}}}$ represents the activations from replay data, $N_{\text{replay}} = |\mathcal{D}_{\text{replay}}^{(t)}|$ is the number of replay samples, and N_{patch} is the number of image patches or tokens.

Once the covariance matrix is computed, we perform singular value decomposition (SVD) on the covariance matrix $C^{(t)}$ multiplied by the linear projection weight W of this layer:

$$\text{SVD}(WC^{(t)}) = U\Sigma V^\top = \sum_{i=1}^R \sigma_i \mathbf{u}_i \mathbf{v}_i^\top, \quad (2)$$

where $W \in \mathbb{R}^{d_{\text{out}} \times d_{\text{in}}}$ is the weight matrix, $\Sigma \in \mathbb{R}^{d_{\text{out}} \times d_{\text{in}}}$ is a diagonal matrix with singular values σ_i arranged in descending order, R is the total number of singular values of $WC^{(t)}$, *i.e.*, $R = \min\{d_{\text{out}}, d_{\text{in}}\}$, and $U \in \mathbb{R}^{d_{\text{out}} \times d_{\text{out}}}$, $V \in \mathbb{R}^{d_{\text{in}} \times d_{\text{in}}}$ are orthogonal matrices containing the left and right singular vectors \mathbf{u}_i and \mathbf{v}_i , respectively.

To preserve existing knowledge while enabling adaptation, we split the decomposed components into two parts:

- **Knowledge-sensitive components:** This part corresponds to the largest singular values (the first $R - r$ components), which dominate the contributions to the previously acquired abilities. These components are frozen during adaptation in the current session to preserve existing knowledge.
- **Redundant-capacity components:** This part consists of components with the smallest r singular values and is used to create learnable adapters for adaptation to new tasks.

The two parts are complementary, and more importantly, the redundant-capacity components minimize interference with the existing abilities as much as possible to ensure both stability for old classes and plasticity for new tasks.

To avoid a large model drift at the start of each session’s adaptation, the inference result needs to remain unchanged. We reconstruct the weight matrix W as:

$$\hat{W} = U\Sigma(V^\top C^{-1}) = \sum_{i=1}^R \sigma_i \mathbf{u}_i \hat{\mathbf{v}}_i^\top, \quad (3)$$

where $\hat{\mathbf{v}}_i^\top$ is the i -th row vector of $V^\top C^{-1}$.

As illustrated in Fig. 2 (b), the redundant-capacity components are used to construct two learnable low-rank matrices, B and A , which serve as learnable adapters to accommodate new tasks:

$$\begin{aligned} W' &= W - BA, \\ B &= U_{[:, -r:]} \sqrt{\Sigma}_{[-r:]}, \\ A &= \sqrt{\Sigma}_{[-r:]} (V^\top C^{-1})_{[-r:;, :]}, \end{aligned} \quad (4)$$

where $U_{[:, -r:]}$ refers to the last r columns of the matrix U , $(V^\top C^{-1})_{[-r:;, :]}$ refers to the last r rows of the matrix $V^\top C^{-1}$, and $\sqrt{\Sigma}_{[-r:]}$ is a diagonal matrix containing the square roots of the smallest r singular values on its diagonal. $B \in \mathbb{R}^{d_{\text{out}} \times r}$ and $A \in \mathbb{R}^{r \times d_{\text{in}}}$ form the low-rank adapter matrices, and $BA = \sum_{i=R-r+1}^R \sigma_i \mathbf{u}_i \hat{\mathbf{v}}_i^\top$ corresponds to the sum of the last r components in Eq. (3). W' corresponds to the knowledge-sensitive components, *i.e.*, the first $R - r$ components in Eq. (3), and we calculate it by $W - BA$ to reduce numerical error. During adaptation, only the parameters in B and A are learnable and updated, while W' remains frozen to preserve previously acquired knowledge.

After fine-tuning, we merge the optimized parameters B^* and A^* back into the frozen components to form the updated weight matrix:

$$W^* = W' + B^* A^*. \quad (5)$$

This ensures that no additional parameter is introduced into the model, maintaining inference efficiency and the original model architecture.

As illustrated in Fig. 2 (c), as the model progresses through sessions, CKPD-FSCIL continuously recalculates the covariance matrix $C^{(t)}$ and reapplies the decomposition process to assimilate new abilities into the knowledge-sensitive components, allowing our method to handle evolving task characteristics in FSCIL. The replay data for session $t + 1$ is updated to include all classes from previous sessions:

$$\mathcal{D}_{\text{replay}}^{(t+1)} = \{(\mathbf{x}_i, y_i) \mid y_i \in \bigcup_{i=0}^t \mathcal{C}^{(i)}\}. \quad (6)$$

3.3. Adaptive Layer Selection via Adapter Sensitivity Evaluation

In CKPD, the model’s weights are decomposed into knowledge-sensitive components and redundant-capacity components. However, not all layers are equally sensitive to existing knowledge or have equal redundant capacity to accommodate new knowledge. Allocating learnable adapters to layers that are highly sensitive to existing knowledge can still lead to catastrophic forgetting, thereby compromising the model’s ability to retain previously learned classes. Additionally, the redundant capacity for new knowledge not only varies across different layers but also changes over incremental sessions. Therefore, it is essential to identify and select the most adaptable layers that have the most redundant capacity and make the minimal contributions to existing abilities.

To address this challenge, we employ a strategy for adaptive layer selection. We introduce a metric, Adapter Sensitivity Ratio (ASR), which quantifies the sensitivity of the detached redundant-capacity components in each layer to existing knowledge. The ASR for a given layer l is calculated as:

$$\text{ASR}^l = \frac{\sigma_{-r}^l}{\sigma_{\min}^l}, \quad (7)$$

where σ_{-r}^l is the r -th last singular value of Σ^l , the diagonal matrix of singular values obtained from the knowledge-preserving decomposition in layer l as defined in Eq. (2). σ_{-r}^l also represents the largest singular value among the redundant-capacity components, while σ_{\min}^l denotes the smallest singular value of the layer.

A lower ASR indicates that the adapter is less likely to interfere with existing knowledge, as these components have singular values that are closer to the smallest one, which means the adapter only contains redundant components. Conversely, a higher ASR indicates that some important components with non-negligible contributions to existing knowledge are included in the adapter. The ASR also shares a similar concept with the matrix condition number.

To minimize interference with existing knowledge and ensure stable adaptation, layers with lower ASR values are prioritized for adapter allocation. As shown in Fig. 2 (d), for

each layer l in session t , the ASR^l value is calculated using the singular values obtained from the knowledge-preserving decomposition. Once the ASR values are computed, all layers are ranked in ascending order of their ASR values as follows:

$$ASR^{l_1^{(t)}} \leq ASR^{l_2^{(t)}} \leq \dots \leq ASR^{l_N^{(t)}}, \quad (8)$$

where $ASR^{l_1^{(t)}}$ represents the smallest ASR and $ASR^{l_N^{(t)}}$ represents the largest. Here, N is the total number of linear layers in the network. As illustrated in Fig. 2 (c), the K layers with the smallest ASR values are selected for adapter allocation:

$$\mathcal{L}_{\text{selected}}^{(t)} = \{l_1^{(t)}, l_2^{(t)}, \dots, l_K^{(t)}\}, \quad (9)$$

where K is the predefined number of layers to adapt in each session. The adapters in the selected layers, $\mathcal{L}_{\text{selected}}^{(t)}$, are trained during the session, while the remaining $N - K$ layers are kept frozen to preserve learned knowledge.

At the start of each incremental session $t + 1$, the covariance matrices $C^{(t+1)}$ are recalculated using the updated replay dataset $\mathcal{D}_{\text{replay}}^{(t+1)}$. Based on these updated matrices, the ASR values are recomputed, and the adaptive layer selection mechanism identifies a new set of K layers for adaptation: $\mathcal{L}_{\text{selected}}^{(t+1)} = \{l_1^{(t+1)}, l_2^{(t+1)}, \dots, l_K^{(t+1)}\}$.

The proposed adaptive layer selection strategy dynamically reallocates adapters in each session and ensures that the most adaptable layers are selected based on the current distribution of redundant capacity across the layers.

3.4. Implementation

In implementations, we use Vision Transformer [11] as the backbone network because the majority of parameterized modules are linear projection layers. After the backbone network, we adopt the Mamba-FSCIL projector [27], which projects the output features through a selective state space module [15], and calculates classification error using the ETF classifier head and the DR loss function [60]. Apart from the loss functions proposed in Mamba-FSCIL for the projector and the DR loss, we do not introduce any loss function in our method. In base session training, the parameters of the last block in the backbone network and the projector are learnable. In incremental sessions, different from Mamba-FSCIL [27] and most existing studies that freeze the backbone network [60], we train the adapters allocated by our method along with the projector, which releases the adaptability of the backbone network while preserving essential components associated with foundational abilities.

4. Experiments

We compare CKPD-FSCIL with state-of-the-art FSCIL methods, including those with frozen backbones and

prompt/token-based adaptation. Additionally, ablation studies are performed to assess the contributions of continuous knowledge-preserving decomposition and adaptive layer selection.

Following the standard experimental settings [27, 36, 47, 54, 60], we conduct experiments on three widely used FSCIL benchmarks, including miniImageNet [42], CIFAR-100 [23], and CUB-200 [51]. We use the image branch of CLIP-ViT-B/16 [38] as the starting backbone following prior works [14, 36, 54]. For dataset and training details, please refer to the Appendix.

4.1. Comparison with the State-of-the-art Methods

As shown in Tables 1 and 2, CKPD-FSCIL consistently outperforms other FSCIL methods on the miniImageNet and CUB-200 datasets. CPE-CLIP [6], CEC+ [53], and KANet [54] use OpenAI CLIP’s image branch [38] for weight initialization.

On miniImageNet, our CKPD-FSCIL achieves 90.66% average accuracy, surpassing CPE-CLIP [6] by 4.53%. Unlike CPE-CLIP, our CKPD-FSCIL improves performance without extra parameters or computational overhead. It also outperforms methods that freeze the backbone, such as Mamba-FSCIL [27] and NC-FSCIL [60], thanks to the enhanced adaptability coming from the redundant-capacity components of our method. With an IN21K pre-trained backbone, our CKPD-FSCIL achieves 95.36% average accuracy, outperforming PriViLege [36] that uses prompts and knowledge distillation. As a comparison, our CKPD-FSCIL achieves superior performance without relying on additional parameters or distillation supervision.

On CUB-200, our CKPD-FSCIL outperforms KANet [54] by 5.83% in terms of average accuracy. It is noteworthy that KANet [54] requires manual tuning and extra parameters. By contrast, our method automatically selects layers for fine-tuning, and more importantly, preserves model structure and inference efficiency, as shown in the comparison in the Appendix. With an IN21K pre-trained backbone, CKPD-FSCIL achieves 84.95% average accuracy, surpassing PriViLege [36], PL-FSCIL [48], and ASP-FSCIL [30], which also add complexity with extra prompts and knowledge distillation.

Comparison with Methods using Pre-trained Models.

Recent advancements in FSCIL leverage pretrained models to adapt to new classes. However, many methods introduce additional parameters, prompts, or modules, increasing model complexity and inference cost. Tab. 3 summarizes key differences between CKPD-FSCIL and other methods. Among them, CPE-CLIP [6] employs extra learnable multimodal prompts for CLIP’s language and vision encoders, adding a regularization loss to ensure stable learning. PriViLege [36] introduces additional base prompts and vision-language prompts to facilitate the incre-

Table 1. FSCIL performance comparison on miniImageNet. “Average Acc.” represents the mean accuracy across all sessions. † indicates models with ImageNet-1K [7] pretraining. †† refers to ImageNet-21K [42] pretraining.

Methods	Venue	Accuracy in each session †										Average
		0	1	2	3	4	5	6	7	8	Acc.	
DSN [59]	TPAMI 2022	68.95	63.46	59.78	55.64	52.85	51.23	48.90	46.78	45.89	54.83	
Data-free [31]	ECCV 2022	71.84	67.12	63.21	59.77	57.01	53.95	51.55	49.52	48.21	58.02	
MetaFSCIL [5]	CVPR 2022	72.04	67.94	63.77	60.29	57.58	55.16	52.90	50.79	49.19	58.85	
LIMIT [69]	TPAMI 2022	72.32	68.47	64.30	60.78	57.95	55.07	52.70	50.72	49.19	59.06	
FACT [68]	CVPR 2022	72.56	69.63	66.38	62.77	60.60	57.33	54.34	52.16	50.49	60.70	
CABD [67]	CVPR 2023	74.65	70.43	66.29	62.77	60.75	57.24	54.79	53.65	52.22	61.42	
TEEN [52]	NeurIPS 2023	73.53	70.55	66.37	63.23	60.53	57.95	55.24	53.44	52.08	61.44	
C-FSCIL [18]	CVPR 2022	76.40	71.14	66.46	63.29	60.42	57.46	54.78	53.11	51.41	61.61	
Regularizer [3]	ICLR 2022	80.37	74.68	69.39	65.51	62.38	59.03	56.36	53.95	51.73	63.71	
ALICE [37]	ECCV 2022	80.60	70.60	67.40	64.50	62.50	60.00	57.80	56.80	55.70	63.99	
SAVC [44]	CVPR 2023	81.12	76.14	72.43	68.92	66.48	62.95	59.92	58.39	57.11	67.05	
NC-FSCIL [60]	ICLR 2023	84.02	76.80	72.00	67.83	66.35	64.04	61.46	59.54	58.31	67.82	
FeSSSS [2]	CVPR 2022	81.50	77.04	72.92	69.56	67.27	64.34	62.07	60.55	58.87	68.23	
Mamba-FSCIL [27]	Arxiv 2024	84.93	80.02	74.61	71.33	69.15	65.62	62.38	60.93	59.36	69.81	
CPE-CLIP [6]	ICCVW 2023	90.23	89.56	87.42	86.80	86.51	85.08	83.43	83.38	82.77	86.13	
CKPD-FSCIL	-	96.18	95.25	92.81	91.73	91.07	89.41	87.02	86.18	86.23	90.66	
PriViLege ^{††} [36]	CVPR 2024	96.68	96.49	95.65	95.54	95.54	94.91	94.33	94.19	94.10	95.27	
CKPD-FSCIL^{††}	-	97.77	96.62	95.21	95.39	95.75	94.87	94.18	94.19	94.27	95.36	

Table 2. FSCIL performance comparison on CUB-200. “Average Acc.” represents the mean accuracy across all sessions. Results marked with * are copied from [54], † indicates models with ImageNet-1K [7] pretraining, and †† refers to ImageNet-21K [42] pretraining.

Methods	Venue	Accuracy in each session †										Average	
		0	1	2	3	4	5	6	7	8	9	10	Acc.
Finetune*	-	82.00	76.72	70.42	60.70	45.24	25.75	21.39	16.84	13.05	11.34	10.39	39.44
Data-free [31]	ECCV 2022	75.90	72.14	68.64	63.76	62.58	59.11	57.82	55.89	54.92	53.58	52.39	61.52
MetaFSCIL [5]	CVPR 2022	75.90	72.41	68.78	64.78	62.96	59.99	58.30	56.85	54.78	53.82	52.64	61.93
FeSSSS [2]	CVPR 2022	79.60	73.46	70.32	66.38	63.97	59.63	58.19	57.56	55.01	54.31	52.98	62.85
DSN [59]	TPAMI 2022	76.06	72.18	69.57	66.68	64.42	62.12	60.16	58.94	56.99	55.10	54.21	63.31
FACT [68]	CVPR 2022	75.90	73.23	70.84	66.13	65.56	62.15	61.74	59.83	58.41	57.89	56.94	64.42
ALICE [37]	ECCV 2022	77.40	72.70	70.60	67.20	65.90	63.40	62.90	61.90	60.50	60.60	60.10	65.75
TEEN [52]	NeurIPS 2023	77.26	76.13	72.81	68.16	67.77	64.40	63.25	62.29	61.19	60.32	59.31	66.63
LIMIT [69]	TPAMI 2022	76.32	74.18	72.68	69.19	68.79	65.64	63.57	62.69	61.47	60.44	58.45	66.67
NC-FSCIL [60]	ICLR 2023	80.45	75.98	72.30	70.28	68.17	65.16	64.43	63.25	60.66	60.01	59.44	67.28
Mamba-FSCIL [27]	Arxiv 2024	80.90	76.26	72.97	70.14	67.83	65.74	65.43	64.12	62.31	62.12	61.65	68.13
CPE-CLIP [6]	ICCVW 2023	81.58	78.52	76.68	71.86	71.52	70.23	67.66	66.52	65.09	64.47	64.60	70.79
CEC+* [53]	TCSVT 2023	82.00	76.68	74.97	72.27	71.37	69.89	68.94	68.38	66.89	67.48	67.12	71.45
KANet [54]	Arxiv 2024	82.00	77.99	76.68	74.25	73.37	71.55	70.66	70.26	69.13	69.65	69.35	73.17
CKPD-FSCIL	-	87.05	82.60	82.27	79.48	76.81	77.14	77.46	77.76	76.51	76.39	75.56	79.00
PL-FSCIL [†] [48]	Arxiv 2024	85.16	85.40	82.75	75.22	77.22	73.25	72.39	70.24	67.97	68.33	69.86	75.25
PriViLege ^{††} [36]	CVPR 2024	82.21	81.25	80.45	77.76	77.78	75.95	75.69	76.00	75.19	75.19	75.08	77.50
ASP-FSCIL [†] [30]	ECCV 2024	87.10	86.00	84.90	83.40	83.60	82.40	82.60	83.00	82.60	83.00	83.50	83.83
CKPD-FSCIL^{††}	-	88.20	86.00	85.74	84.58	84.19	83.47	84.31	84.67	84.29	84.56	84.48	84.95

mental transfer of domain-specific and positive knowledge across sessions. It further employs entropy-based divergence loss and semantic knowledge distillation from a pre-trained language model. **PL-FSCIL** [48] utilizes additional visual prompts with a pre-trained ViT, introducing domain and task-specific prompts, and implements an extra prompt regularization mechanism to enforce orthogonality between them. **ASP-FSCIL** [30] proposes an attention-aware self-

adaptive prompt framework using additional task-invariant and task-specific prompts to capture shared and specific knowledge, introducing an extra information bottleneck learning objective. **FSPT-FSCIL** [39] draws inspiration from the brain’s complementary learning systems, introducing additional prompts categorized into fast-update and slow-update groups trained via meta-learning. **KANet** [54] introduces additional knowledge adapter modules to fuse

Table 3. Comparison of CKPD-FSCIL with other methods using pretrained models, highlighting key differences in additional parameters, inference cost, supervision requirements, and layer selection strategies.

Methods	No Additional Parameters	No Additional Inference Cost	No Additional Supervision	Layer Selection Strategy
CPE-CLIP [6]	×	×	×	Manual
PriViLege [36]	×	×	×	Manual
PL-FSCIL [48]	×	×	×	Manual
ASP-FSCIL [30]	×	×	×	Manual
FSPT-FSCIL [39]	×	×	✓	Manual
KANet [54]	×	×	✓	Manual
CKPD-FSCIL	✓	✓	✓	Adaptive

Table 4. Comparison of FLOPs (G) and Parameters (M) across sessions for different methods. Red arrows and numbers indicate the increment relative to the initial pre-trained model (Init).

Methods	FLOPs (Init)	FLOPs (Session 1 ~ Session 8)
PriViLege [36]	85.799	85.810 (↑ 0.01%)
ASP-FSCIL [30]	85.799	173.923 (↑ 102.71%)
CPKD-FSCIL (ours)	85.799	85.799

Methods	Params (Init)	Params (Session 1 ~ Session 8)
PriViLege [36]	17.582	17.766 (↑ 1.05%)
ASP-FSCIL [30]	17.582	35.742 (↑ 103.29%)
CPKD-FSCIL (ours)	17.582	17.582

data-specific knowledge into the general representation.

In contrast, **CKPD-FSCIL** offers several advantages:

(1) No additional parameters or inference cost: CKPD-FSCIL does not introduce extra parameters or computational overhead during inference. By decomposing model weights into knowledge-sensitive components and adaptable redundant-capacity components, and then merging adapters back into the preserved weights, it maintains the original model architecture. **(2) No additional supervision:** CKPD-FSCIL operates without requiring extra supervision for external models or prompts, simplifying the training process. **(3) Adaptive layer selection strategy:** CKPD-FSCIL employs an adaptive layer selection strategy that automatically allocates capacity across layers for new knowledge based on each layer’s sensitivity, eliminating the need for manual layer selection.

Comparison of model complexity. We compare the floating point operations (FLOPs) and parameters of the backbone network during inference for three methods, including CKPD-FSCIL (Ours), PriViLege [36], and ASP-FSCIL [30], across incremental sessions. The initial model (*Init*) refers to the original pre-trained backbone network before incremental training. We indicate the increment ratio compared to the initial model using red arrows and numbers. As shown in Tab. 4, CKPD-FSCIL maintains constant FLOPs and parameters across all sessions, as we do not introduce additional modules or parameters during incremental learning. In contrast, PriViLege and ASP-FSCIL increase both FLOPs and parameters due to the incorporation of prompts and additional modules. Specifically,

Table 5. Performance comparison of CKPD and KPD on the average accuracies across sessions in CIFAR-100 and CUB-200 datasets.

Methods	CIFAR-100	CUB-200
KPD	69.15	76.02
CKPD	71.33	77.98

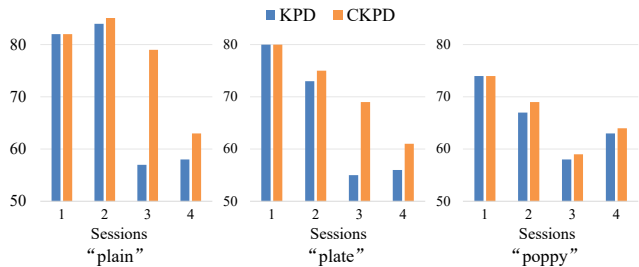


Figure 3. Comparison of CKPD and KPD on accuracy across sessions for novel classes "plain," "plate," and "poppy" from CIFAR-100’s first incremental session.

ASP-FSCIL nearly doubles the number of parameters from 17.582 M to 35.742 M, and the FLOPs also double accordingly. PriViLege also shows a slight increment, in both parameters and FLOPs. These increments lead to higher computational cost and memory requirements during inference, which could be unbearable if continual training lasts for a large number of sessions.

4.2. Ablation Studies

Effect of Continuous Decomposition. We introduce a baseline, denoted as KPD, which performs decomposition only once based on replay data of the base classes, while our CKPD continuously assimilates new abilities into the knowledge-preserving components. We compare CKPD with KPD to assess the impact of continuous decomposition on performance and knowledge retention. Training was performed on CIFAR-100 and CUB-200, with results shown in Tab. 5. CKPD outperforms KPD, achieving 71.33% accuracy on CIFAR-100 (2.18% improvement) and 77.98% on CUB-200 (1.96% improvement), demonstrating better adaptability and overall performance.

Fig. 3 provides a further comparison between CKPD

Table 6. Performance comparison of CKPD-FSCIL with other adaptation methods on CIFAR-100 and CUB-200 datasets. AVG denotes the average accuracy across all sessions. $\text{FINAL}_{\text{Base}}$ denotes the base class accuracy in the final incremental session.

Methods	CIFAR-100		CUB-200	
	AVG \uparrow	$\text{FINAL}_{\text{Base}}\uparrow$	AVG \uparrow	$\text{FINAL}_{\text{Base}}\uparrow$
Freeze	74.76	79.63	77.77	82.93
Full Adapt	73.14	77.80	73.19	77.97
SVD	75.42	78.85	78.44	82.86
ASVD [62]	74.11	75.82	77.63	81.08
LoRA [20]	75.21	78.93	78.35	81.63
CKPD-FSCIL	76.01	80.65	79.21	83.66

Table 7. Performance comparison of different decomposition methods on base class accuracy in CIFAR-100 with varying dropout rates.

Methods	Dropout Rate			
	0.2	0.4	0.6	0.8
SVD	85.92	84.39	75.93	55.18
ASVD	86.10	84.50	76.17	52.10
CKPD	86.17	85.02	77.98	58.53

and KPD, highlighting CKPD’s superior ability to retain performance on novel classes. Specifically, we compare CKPD and KPD on accuracy across sessions for CIFAR-100’s novel classes (“plain”, “plate”, and “poppy” from the first incremental session). CKPD reduces catastrophic forgetting and better retains accuracy for these classes due to its continuous update of the knowledge-preserving components, while KPD, which decomposes only once, cannot mitigate the novel classes’ forgetting.

Effect of Adaptation Methods. We compare CKPD-FSCIL with different adaptation methods on CIFAR-100 and CUB-200 datasets, as shown in Tab. 6. CKPD-FSCIL achieves the highest average accuracies of 76.01% on CIFAR-100 and 79.21% on CUB-200, along with the highest last-session base accuracies of 80.65% and 83.66%, outperforming other methods. CKPD-FSCIL outperforms SVD, ASVD, and LoRA by dynamically separating redundant components from essential knowledge, fine-tuning only the redundant parts. Unlike ASVD’s incorporating activation mean values, CKPD uses covariance-based decomposition to better capture discriminative components, leading to superior performance.

Additionally, when varying dropout rates are applied to the adapter with rank of 640, CKPD shows the slowest decline in base accuracy, as shown in Tab. 7. The results indicate that the adapter built by our CKPD has the least interference with the knowledge to maintain, highlighting its superior ability to concentrate existing knowledge into the principal components.

Effect of Adaptive Layer Selection. We compare the adaptive layer selection method with manual strategies on

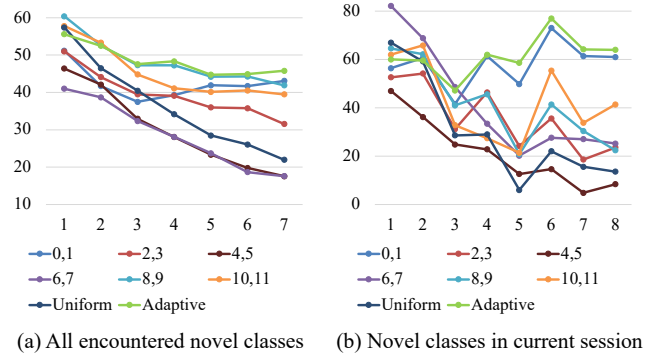


Figure 4. Comparison of adaptive vs. manual layer selection in CKPD-FSCIL on CIFAR-100. (a) Average accuracy on previously learned novel classes. (b) Performance on the newly added novel classes after each session. “Adaptive” refers to your adaptive layer selection. “Uniform” is uniformly selecting 6 layers with 1 adapter for each layer. The other choices are manually selecting 2 layers with 3 adapters for each layer.

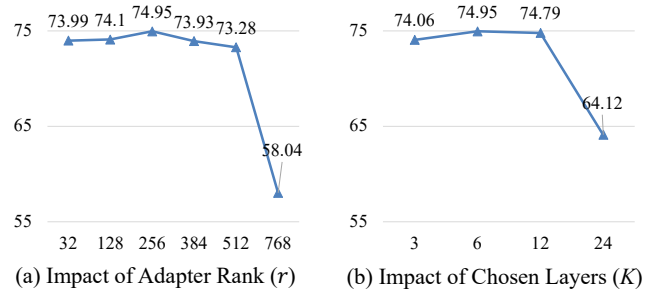


Figure 5. Impact of adapter rank r and adaptable layers K : (a) on r and (b) on K .

CIFAR-100, including manually selecting two layers (*e.g.*, layer indices of $\{0, 1\}$ or $\{8, 9\}$) with 3 adapters for each layer uniformly selecting 6 layers (the layer indices of $\{0, 2, 4, 6, 8, 10\}$) with 1 adapter for each layer.

As shown in Fig. 4, our adaptive layer selection (“Adaptive” in the figure) outperforms manual strategies in both learning novel classes in the current session while maintaining all novel classes encountered. Manual selection (8,9) performs similarly with ours in Fig. 4-(a), but lags behind in adapting to new classes. Manual selection (8,9) performs well in Fig. 4-(b), but is inferior to ours in Fig. 4-(a). It implies that our adaptive layer selection method can allocate adapters for both knowledge retention and task adaptation, outperforming manual methods in both aspects.

Impact of Adapter Rank r and Number of Adaptable Layers K We evaluate the impact of adapter rank r and the number of adaptable layers K on CIFAR-100. As shown in Fig. 5 (a), peak performance occurs at $r = 256$, with accuracy declining as r increases. Although performance remains strong at $r = 512$, it drops significantly at $r = 768$, which corresponds to full fine-tuning. It indicates that catastrophic forgetting occurs when full fine-tuning, and using

our method with adapter rank in a proper range will have stable performance. In Fig. 5 (b), the best performance is observed at $N = 6$, with only slight degradation at $N = 12$. However, when $N = 24$, performance drops noticeably, suggesting that adapting too many layers also degrades model performance. Overall, CKPD-FSCIL effectively balances adaptability and knowledge retention across a range of r and K choices.

5. Conclusion

In this paper, we propose CKPD-FSCIL, which offers an efficient solution to the challenges of FSCIL by decoupling model weights into knowledge-preserving and adaptable components. By freezing knowledge-sensitive components and adapting redundant capacity, our framework strikes a balance between retaining prior knowledge and learning new tasks. The adaptive layer selection strategy further enhances this balance, dynamically allocating adapters based on adapter sensitivity. Our method does not rely on additional modules or prompts that introduce extra inference overhead. Experimental results on multiple benchmarks show that CKPD-FSCIL outperforms current state-of-the-art methods, demonstrating its effectiveness in mitigating catastrophic forgetting while maintaining adaptability.

Limitations and future work. The adaptive layer selection strategy proposed by our method is able to automatically assign adapters across layers. But we adopt the same adapter rank for all selected layers. Different layers may contain various available capacities for new knowledge. Therefore, developing an adaptive rank allocation strategy may further enhance the ability to preserve existing knowledge without sacrificing adaptability, which deserves our future exploration.

References

- [1] Aishwarya Agarwal, Biplab Banerjee, Fabio Cuzzolin, and Subhasis Chaudhuri. Semantics-driven generative replay for few-shot class incremental learning. In *ACM MM*, 2022. 2, 3
- [2] Touqeer Ahmad, Akshay Raj Dhamija, Steve Cruz, Ryan Rabinowitz, Chunchun Li, Mohsen Jafarzadeh, and Terrance E. Boult. Few-shot class incremental learning leveraging self-supervised features. In *CVPR*, 2022. 7, 2
- [3] Afra Feyza Akyürek, Ekin Akyürek, Derry Wijaya, and Jacob Andreas. Subspace regularizers for few-shot class incremental learning. In *ICLR*, 2022. 7
- [4] Ali Cheraghian, Shafin Rahman, Pengfei Fang, Soumava Kumar Roy, Lars Petersson, and Mehrtash Harandi. Semantic-aware knowledge distillation for few-shot class-incremental learning. In *CVPR*, 2021. 3
- [5] Zhixiang Chi, Li Gu, Huan Liu, Yang Wang, Yuanhao Yu, and Jin Tang. Metafscil: A meta-learning approach for few-shot class incremental learning. In *CVPR*, 2022. 7, 2
- [6] Marco D’Alessandro, Alberto Alonso, Enrique Calabrés, and Mikel Galar. Multimodal parameter-efficient few-shot class incremental learning. In *ICCV*, 2023. 2, 3, 6, 7, 8
- [7] Jia Deng, Wei Dong, Richard Socher, Li-Jia Li, Kai Li, and Li Fei-Fei. Imagenet: A large-scale hierarchical image database. In *CVPR*, 2009. 7, 2
- [8] Terrance DeVries. Improved regularization of convolutional neural networks with cutout. *arXiv preprint arXiv:1708.04552*, 2017. 1
- [9] Ning Ding, Yujia Qin, Guang Yang, Fuchao Wei, Zonghan Yang, Yusheng Su, Shengding Hu, Yulin Chen, Chi-Min Chan, Weize Chen, et al. Parameter-efficient fine-tuning of large-scale pre-trained language models. *Nature Machine Intelligence*, 2023. 3
- [10] Songlin Dong, Xiaopeng Hong, Xiaoyu Tao, Xinyuan Chang, Xing Wei, and Yihong Gong. Few-shot class-incremental learning via relation knowledge distillation. In *AAAI*, 2021. 3
- [11] Alexey Dosovitskiy, Lucas Beyer, Alexander Kolesnikov, Dirk Weissenborn, Xiaohua Zhai, Thomas Unterthiner, Mostafa Dehghani, Matthias Minderer, Georg Heigold, Sylvain Gelly, et al. An image is worth 16x16 words: Transformers for image recognition at scale. In *ICLR*, 2020. 6, 1
- [12] Ronald A Fisher. The use of multiple measurements in taxonomic problems. *Annals of eugenics*, 1936. 2
- [13] Ian J Goodfellow, Mehdi Mirza, Da Xiao, Aaron Courville, and Yoshua Bengio. An empirical investigation of catastrophic forgetting in gradient-based neural networks. *arXiv preprint arXiv:1312.6211*, 2013. 1, 3
- [14] Dipam Goswami, Bartłomiej Twardowski, and Joost Van De Weijer. Calibrating higher-order statistics for few-shot class-incremental learning with pre-trained vision transformers. In *CVPR*, 2024. 2, 3, 6, 1
- [15] Albert Gu and Tri Dao. Mamba: Linear-time sequence modeling with selective state spaces. *arXiv preprint arXiv:2312.00752*, 2023. 6
- [16] Hangfeng He and Weijie J Su. A law of data separation in deep learning. *National Academy of Sciences*, 2023. 2
- [17] Junxian He, Chunting Zhou, Xuezhe Ma, Taylor Berg-Kirkpatrick, and Graham Neubig. Towards a unified view of parameter-efficient transfer learning. In *ICLR*, 2022. 3
- [18] Michael Hersche, Geethan Karunaratne, Giovanni Cherubini, Luca Benini, Abu Sebastian, and Abbas Rahimi. Constrained few-shot class-incremental learning. In *CVPR*, 2022. 2, 3, 7
- [19] Neil Houlsby, Andrei Giurgiu, Stanislaw Jastrzebski, Bruna Morrone, Quentin De Laroussilhe, Andrea Gesmundo, Mona Attariyan, and Sylvain Gelly. Parameter-efficient transfer learning for nlp. In *ICML*, 2019. 3
- [20] Edward J Hu, Yelong Shen, Phillip Wallis, Zeyuan Allen-Zhu, Yuanzhi Li, Shean Wang, Lu Wang, and Weizhu Chen. LoRA: Low-rank adaptation of large language models. In *ICLR*, 2022. 3, 9
- [21] Menglin Jia, Luming Tang, Bor-Chun Chen, Claire Cardie, Serge Belongie, Bharath Hariharan, and Ser-Nam Lim. Visual prompt tuning. In *ECCV*, 2022. 3

- [22] KJ Joseph, Salman Khan, Fahad Shahbaz Khan, Rao Muhammad Anwer, and Vineeth N Balasubramanian. Energy-based latent aligner for incremental learning. In *CVPR*, 2022. 2, 3
- [23] Alex Krizhevsky. Learning multiple layers of features from tiny images. 2009. 6
- [24] Anna Kukleva, Hilde Kuehne, and Bernt Schiele. Generalized and incremental few-shot learning by explicit learning and calibration without forgetting. In *ICCV*, 2021. 3
- [25] Tao Lei, Junwen Bai, Siddhartha Brahma, Joshua Ainslie, Kenton Lee, Yanqi Zhou, Nan Du, Vincent Y Zhao, Yuxin Wu, Bo Li, et al. Conditional adapters: Parameter-efficient transfer learning with fast inference. In *NeurIPS*, 2023. 3
- [26] Brian Lester, Rami Al-Rfou, and Noah Constant. The power of scale for parameter-efficient prompt tuning. In *EMNLP*, 2021. 3
- [27] Xiaojie Li, Yibo Yang, Jianlong Wu, Bernard Ghanem, Liqiang Nie, and Min Zhang. Mamba-fscil: Dynamic adaptation with selective state space model for few-shot class-incremental learning. *arXiv preprint arXiv:2407.06136*, 2024. 2, 3, 6, 7, 1
- [28] Xiang Lisa Li and Percy Liang. Prefix-tuning: Optimizing continuous prompts for generation. In *IJCNLP*, 2021. 3
- [29] Zhizhong Li and Derek Hoiem. Learning without forgetting. *TPAMI*, 2017. 1, 3
- [30] Chenxi Liu, Zhenyi Wang, Tianyi Xiong, Ruibo Chen, Yihan Wu, Junfeng Guo, and Heng Huang. Few-shot class incremental learning with attention-aware self-adaptive prompt. *arXiv preprint arXiv:2403.09857*, 2024. 2, 3, 6, 7, 8
- [31] Huan Liu, Li Gu, Zhixiang Chi, Yang Wang, Yuanhao Yu, Jun Chen, and Jin Tang. Few-shot class-incremental learning via entropy-regularized data-free replay. In *ECCV*, 2022. 2, 3, 7
- [32] Bin Lu, Xiaoying Gan, Lina Yang, Weinan Zhang, Luoyi Fu, and Xinbing Wang. Geometer: Graph few-shot class-incremental learning via prototype representation. In *ACM MM*, 2022. 2, 3
- [33] Michael McCloskey and Neal J Cohen. *Catastrophic interference in connectionist networks: The sequential learning problem*. Elsevier, 1989. 1, 3
- [34] Geoffrey J McLachlan. *Discriminant analysis and statistical pattern recognition*. John Wiley & Sons, 2005. 2
- [35] Martial Mermillod, Aurélie Bugaiska, and Patrick Bonin. The stability-plasticity dilemma: Investigating the continuum from catastrophic forgetting to age-limited learning effects, 2013. 2, 3
- [36] Keon-Hee Park, Kyungwoo Song, and Gyeong-Moon Park. Pre-trained vision and language transformers are few-shot incremental learners. In *CVPR*, 2024. 2, 3, 6, 7, 8, 1
- [37] Can Peng, Kun Zhao, Tianren Wang, Meng Li, and Brian C Lovell. Few-shot class-incremental learning from an open-set perspective. In *ECCV*, 2022. 2, 3, 7
- [38] Alec Radford, Jong Wook Kim, Chris Hallacy, Aditya Ramesh, Gabriel Goh, Sandhini Agarwal, Girish Sastry, Amanda Askell, Pamela Mishkin, Jack Clark, et al. Learning transferable visual models from natural language supervision. In *ICML*, 2021. 6, 1
- [39] Hang Ran, Xingyu Gao, Lusi Li, Weijun Li, Songsong Tian, Gang Wang, Hailong Shi, and Xin Ning. Brain-inspired fast-and slow-update prompt tuning for few-shot class-incremental learning. *TNNLS*, 2024. 2, 3, 7, 8
- [40] Sachin Ravi and Hugo Larochelle. Optimization as a model for few-shot learning. In *ICLR*, 2017. 1, 3
- [41] Sylvestre-Alvise Rebuffi, Alexander Kolesnikov, Georg Sperl, and Christoph H Lampert. icarl: Incremental classifier and representation learning. In *CVPR*, 2017. 1, 3
- [42] Olga Russakovsky, Jia Deng, Hao Su, Jonathan Krause, Sanjeev Satheesh, Sean Ma, Zhiheng Huang, Andrej Karpathy, Aditya Khosla, Michael Bernstein, et al. Imagenet large scale visual recognition challenge. *IJCV*, 2015. 6, 7, 2
- [43] Jake Snell, Kevin Swersky, and Richard Zemel. Prototypical networks for few-shot learning. In *NeurIPS*, 2017. 1, 3
- [44] Zeyin Song, Yifan Zhao, Yujun Shi, Peixi Peng, Li Yuan, and Yonghong Tian. Learning with fantasy: Semantic-aware virtual contrastive constraint for few-shot class-incremental learning. In *CVPR*, 2023. 7
- [45] Flood Sung, Yongxin Yang, Li Zhang, Tao Xiang, Philip H. S. Torr, and Timothy M. Hospedales. Learning to compare: Relation network for few-shot learning. In *CVPR*, 2018. 1, 3
- [46] Xiaoyu Tao, Xinyuan Chang, Xiaopeng Hong, Xing Wei, and Yihong Gong. Topology-preserving class-incremental learning. In *ECCV*, 2020. 2, 3
- [47] Xiaoyu Tao, Xiaopeng Hong, Xinyuan Chang, Songlin Dong, Xing Wei, and Yihong Gong. Few-shot class-incremental learning. In *CVPR*, 2020. 1, 2, 3, 6
- [48] Songsong Tian, Lusi Li, Weijun Li, Hang Ran, Li Li, and Xin Ning. Pl-fscil: Harnessing the power of prompts for few-shot class-incremental learning. *arXiv preprint arXiv:2401.14807*, 2024. 2, 3, 6, 7, 8
- [49] Songsong Tian, Lusi Li, Weijun Li, Hang Ran, Xin Ning, and Prayag Tiwari. A survey on few-shot class-incremental learning. *Neural Networks*, 2024. 1, 3
- [50] Oriol Vinyals, Charles Blundell, Timothy Lillicrap, and Daan Wierstra. Matching networks for one shot learning. In *NeurIPS*, 2016. 1, 3
- [51] Catherine Wah, Steve Branson, Peter Welinder, Pietro Perona, and Serge Belongie. The caltech-ucsd birds-200-2011 dataset. 2011. 6
- [52] Qi-Wei Wang, Da-Wei Zhou, Yi-Kai Zhang, De-Chuan Zhan, and Han-Jia Ye. Few-shot class-incremental learning via training-free prototype calibration. In *NeurIPS*. MIT Press, 2024. 7, 1, 2
- [53] Ye Wang, Guoshuai Zhao, and Xueming Qian. Improved continually evolved classifiers for few-shot class-incremental learning. *TCSVT*, 2023. 2, 3, 6, 7
- [54] Ye Wang, Yaxiong Wang, Guoshuai Zhao, and Xueming Qian. Knowledge adaptation network for few-shot class-incremental learning. *arXiv preprint arXiv:2409.11770*, 2024. 2, 3, 6, 7, 8, 1
- [55] Zifeng Wang, Zizhao Zhang, Sayna Ebrahimi, Ruoxi Sun, Han Zhang, Chen-Yu Lee, Xiaoqi Ren, Guolong Su, Vincent Perot, Jennifer Dy, et al. Dualprompt: Complementary prompting for rehearsal-free continual learning. In *ECCV*, 2022. 3

- [56] Lingling Xu, Haoran Xie, Si-Zhao Joe Qin, Xiaohui Tao, and Fu Lee Wang. Parameter-efficient fine-tuning methods for pretrained language models: A critical review and assessment. *arXiv preprint arXiv:2312.12148*, 2023. 3
- [57] Shipeng Yan, Jiangwei Xie, and Xuming He. Der: Dynamically expandable representation for class incremental learning. In *CVPR*, 2021. 2, 3
- [58] Boyu Yang, Mingbao Lin, Binghao Liu, Mengying Fu, Chang Liu, Rongrong Ji, and Qixiang Ye. Learnable expansion-and-compression network for few-shot class-incremental learning. *arXiv preprint arXiv:2104.02281*, 2021.
- [59] Boyu Yang, Mingbao Lin, Yunxiao Zhang, Binghao Liu, Xiaodan Liang, Rongrong Ji, and Qixiang Ye. Dynamic support network for few-shot class incremental learning. *TPAMI*, 2022. 2, 3, 7
- [60] Yibo Yang, Haobo Yuan, Xiangtai Li, Zhouchen Lin, Philip Torr, and Dacheng Tao. Neural collapse inspired feature-classifier alignment for few-shot class-incremental learning. In *ICLR*, 2023. 2, 3, 6, 7, 1
- [61] Yibo Yang, Xiaojie Li, Zhongzhu Zhou, Shuaiwen Leon Song, Jianlong Wu, Liqiang Nie, and Bernard Ghanem. Corda: Context-oriented decomposition adaptation of large language models. *arXiv preprint arXiv:2406.05223*, 2024. 1, 3
- [62] Zhihang Yuan, Yuzhang Shang, Yue Song, Qiang Wu, Yan Yan, and Guangyu Sun. Asvd: Activation-aware singular value decomposition for compressing large language models. *arXiv preprint arXiv:2312.05821*, 2023. 9
- [63] Chi Zhang, Nan Song, Guosheng Lin, Yun Zheng, Pan Pan, and Yinghui Xu. Few-shot incremental learning with continually evolved classifiers. In *CVPR*, 2021. 2, 3
- [64] H Zhang, M Cisse, Y Dauphin, and D Lopez-Paz. mixup: Beyond empirical risk management. In *ICLR*, 2018. 1
- [65] Jinghua Zhang, Li Liu, Olli Silven, Matti Pietikäinen, and Dewen Hu. Few-shot class-incremental learning: A survey. *arXiv preprint arXiv:2308.06764*, 2023. 1, 3
- [66] Qingru Zhang, Minshuo Chen, Alexander Bukharin, Pengcheng He, Yu Cheng, Weizhu Chen, and Tuo Zhao. Adaptive budget allocation for parameter-efficient fine-tuning. In *ICLR*, 2023. 3
- [67] Linglan Zhao, Jing Lu, Yunlu Xu, Zhanzhan Cheng, Dashan Guo, Yi Niu, and Xiangzhong Fang. Few-shot class-incremental learning via class-aware bilateral distillation. In *CVPR*, 2023. 7, 2
- [68] Da-Wei Zhou, Fu-Yun Wang, Han-Jia Ye, Liang Ma, Shiliang Pu, and De-Chuan Zhan. Forward compatible few-shot class-incremental learning. In *CVPR*, 2022. 7, 2
- [69] Da-Wei Zhou, Han-Jia Ye, Liang Ma, Di Xie, Shiliang Pu, and De-Chuan Zhan. Few-shot class-incremental learning by sampling multi-phase tasks. *TPAMI*, 2022. 7, 2
- [70] Yixiong Zou, Shanghang Zhang, Yuhua Li, Ruixuan Li, et al. Compositional few-shot class-incremental learning. In *ICML*, 2024. 2, 3

Continuous Knowledge-Preserving Decomposition for Few-Shot Continual Learning

Supplementary Material

A. Implementation Details

Datasets. miniImageNet consists of 100 classes, each having 500 training and 100 testing images of 84×84 pixels. CIFAR-100 has the same number of classes and images, and the image size is 32×32 . CUB-200 is a fine-grained classification dataset consisting of 11,788 images in 200 classes, with an image resolution of 224×224 . For miniImageNet and CIFAR-100, the base session includes 60 classes, followed by 8 incremental sessions with a 5-way 5-shot setup (5 classes with 5 images per class). For CUB-200, the base session includes 100 classes, followed by 10 incremental sessions in a 10-way 5-shot setting.

Training Details. We conduct experiments using PyTorch on 8 NVIDIA A100-SXM4 (40GB) GPUs. Following prior works [14, 36, 54], we adopt the image branch of CLIP-ViT-B/16 [38] as our backbone, initializing weights from the pre-trained model provided by OpenAI.¹ For experiments with models pre-trained on ImageNet-21K, we initialize weights from the PyTorch Image Models repository² using the pre-trained weights provided³, following the setup in [36, 52]. For consistency across datasets, input images are resized to 224×224 and are processed through standard data augmentations, including random resizing, flipping, color jittering, Mixup [64], and Cutout [8], as in [27, 60].

In the base session, only the last block of ViT-B [11] is fully trainable, while all the other layers are frozen to preserve generalization capabilities. CKPD-FSCIL is applied during incremental sessions to adapt to new knowledge without interfering with existing abilities. Across all sessions and datasets, we use a batch size of 128, combining new session data with replay data and features (one sample per class). Other training details are as follows:

- **Base Session Training:** We train for 200 epochs on all datasets. The initial learning rates are set to 0.25 for miniImageNet and CIFAR-100, and 0.2 for CUB-200.
- **Incremental Sessions:** Each incremental session consists of 1000 iterations across all datasets. The initial learning rates are 0.1 for miniImageNet, 0.25 for CIFAR-100, and

0.05 for CUB-200. For stability, the adapter’s learning rate is set to 10% of the projector’s learning rate. The adapter rank r (defined in Eq. (4) in the main paper) is set to 128 for miniImageNet and CUB-200, and 256 for CIFAR-100. The number of adaptively selected layers K (introduced in Sec. 3.3) is set to 6 for all datasets.

B. More Results

Comparison with the state-of-the-art methods on CIFAR-100. Due to space constraints in the main text, we show the performance comparison of CKPD-FSCIL with state-of-the-art methods on the CIFAR-100 dataset in Tab. 8 in the Appendix. For a fair comparison, we integrate our proposed CKPD-FSCIL method into the PriViLege framework [36], which is based on ViT models pretrained on ImageNet-21K. We train the base session for 20 epochs and each incremental session for 20 epochs, setting the initial learning rates to $2e-4$ and $5e-5$, respectively.

Our method achieves an average accuracy of **88.62%**, which is a 0.21% improvement over PriViLege’s 88.41%. CKPD-FSCIL consistently surpasses PriViLege across all incremental sessions, highlighting its ability to enhance existing frameworks seamlessly without modifying their structures or adding complexity. Notably, CKPD-FSCIL achieves performance comparable to ASP-FSCIL while avoiding the significant additional computational and parameter cost associated with ASP-FSCIL as demonstrated in Tab. 3 and Tab. 4.

¹<https://huggingface.co/openai/clip-vit-base-patch16>

²<https://github.com/huggingface/pytorch-image-models/>

³https://storage.googleapis.com/vit_models/augreg/B_16-i21k-300ep-lr_0.001-aug_medium1-wd_0.1-do_0.0-sd_0.0--imagenet2012-steps_20k-lr_0.01-res_224.npz

Table 8. FSCIL performance comparison on CIFAR-100. “Average Acc.” denotes the mean accuracy across all sessions. Results marked with * are sourced from [54], † indicates models pre-trained on ImageNet-1K[7], †† indicates models pre-trained on ImageNet-21K [42], and ‡ indicates results reproduced using their official code.

Methods	Venue	Accuracy in each session \uparrow										Average Acc.
		0	1	2	3	4	5	6	7	8		
DSN [59]	TPAMI 2022	73.00	68.83	64.82	62.24	59.16	56.96	54.04	51.57	49.35	60.00	
Data-free [31]	ECCV 2022	74.40	70.20	66.54	62.51	59.71	56.58	54.52	52.39	50.14	60.78	
MetaFSCIL [5]	CVPR 2022	74.50	70.10	66.84	62.77	59.48	56.52	54.36	52.56	49.97	60.79	
FeSSSS [2]	CVPR 2022	75.35	70.81	66.70	62.73	59.62	56.45	54.33	52.10	50.23	60.92	
C-FSCIL [18]	CVPR 2022	77.47	72.40	67.47	63.25	59.84	56.95	54.42	52.47	50.47	61.64	
LIMIT [69]	TPAMI 2022	73.81	72.09	67.87	63.89	60.70	57.77	55.67	53.52	51.23	61.84	
FACT [68]	CVPR 2022	74.60	72.09	67.56	63.52	61.38	58.36	56.28	54.24	52.10	62.24	
TEEN [52]	NeurIPS 2023	74.92	72.65	68.74	65.01	62.01	59.29	57.90	54.76	52.64	63.10	
ALICE [37]	ECCV 2022	79.00	70.50	67.10	63.40	61.20	59.20	58.10	56.30	54.10	63.21	
CABD [67]	CVPR 2023	79.45	75.38	71.84	67.95	64.96	61.95	60.16	57.67	55.88	66.14	
NC-FSCIL [60]	ICLR 2023	82.52	76.82	73.34	69.68	66.19	62.85	60.96	59.02	56.11	67.50	
Mamba-FSCIL [27]	Arxiv 2024	82.80	77.85	73.69	69.67	66.89	63.66	61.48	59.74	57.51	68.14	
Finetune*	-	85.67	81.14	75.37	59.68	50.31	24.00	21.03	16.29	16.85	47.82	
CEC+* [53]	TCSVT 2023	85.67	78.55	76.51	73.80	72.92	71.67	71.76	70.55	68.90	74.48	
KANet [54]	Arxiv 2024	85.67	79.94	78.06	75.43	74.43	73.11	73.16	71.95	70.22	75.77	
CPE-CLIP [6]	ICCVW 2023	87.83	85.86	84.93	82.85	82.64	82.42	82.27	81.44	80.52	83.42	
PL-FSCIL [†] [48]	Arxiv 2024	89.93	77.26	76.12	68.06	69.53	68.21	70.03	69.07	65.73	72.66	
PriViLege ^{††,‡} [36]	CVPR 2024	91.57	89.91	89.66	88.21	88.33	87.44	87.59	87.12	85.84	88.41	
ASP-FSCIL ^{†,‡} [30]	ECCV 2024	91.65	90.22	89.71	88.49	88.56	87.75	87.68	87.34	86.21	88.62	
CKPD-FSCIL ^{††}	-	91.57	90.03	89.84	88.44	88.58	87.74	87.82	87.36	86.22	88.62	